

Statistical ray tracing in plasmas with random density fluctuations

R. Epstein and R. S. Craxton

Laboratory for Laser Energetics, University of Rochester, 250 East River Road, Rochester, New York 14623-1299

(Received 30 August 1985)

The propagation of light rays in a plasma is considered for small density fluctuations superimposed upon a given background density profile. The lowest-order angular spreading, focusing, and drift effects are calculated in the geometrical-optics limit using a statistical random-walk approach. This method is an economical semianalytic alternative to a purely numerical ray-trace approach and is of particular but not exclusive interest in describing the propagation of laser light in laser-produced plasmas. The model is applied to a simple fluctuation spectrum characterized by an rms amplitude and by a correlation length. Results are presented for the evolution of the intensity profiles of beams incident on a plane-parallel linear-profile plasma slab as a function of the angle of incidence. Comparisons of these results with numerical Monte Carlo ray-trace solutions show good agreement. Density fluctuations as small as a few percent of the critical density can, for example, produce significant angular broadening in the specularly reflected beam and reduce the sensitivity of the absorption fraction to the incidence angle, particularly near normal incidence.

I. INTRODUCTION

Statistical ray tracing is a method of describing the random behavior of light rays in a plasma in terms of the statistical properties of the random electron density component. As in the earliest random-medium propagation formalisms, this method is based on the use of geometrical optics to sample the random density fluctuations with light rays.¹⁻³

The random-walk spreading of beams of light due to random density fluctuations is of interest to laser fusion⁴ because, for example, spreading reduces small-scale illumination nonuniformities and because the efficiencies of various energy absorption mechanisms lose some of their angle-of-incidence dependence as the beam acquires a wider angular distribution. Such considerations could affect the spherical uniformity of the deposition of laser energy in the target, which is a crucial quality factor in the success of high-compression implosions.⁵ The results of virtually any laser-plasma interaction experiment where properties of reflected or transmitted light are being measured are bound to be affected at some level by random density fluctuations. The use of the spreading of transmitted or reflected laser beams as a corona-structure diagnostic would not be without precedent; Chandrasekhar was among the first to use the random motion and scintillation of stellar images to obtain estimates of the relevant scale lengths and density fluctuation amplitudes of the turbulent atmospheric layer causing this behavior.¹

The theory of wave propagation in random media has advanced beyond the geometrical-optics formalisms^{2,3,6} and has been applied to ionospheric scattering⁷ and marine acoustics.⁸ Even though the primary concern of this paper is laser-produced plasmas, it should be noted that the work to be described is applicable to wave propagation in random media in other physical contexts.

An important result of this work is the extension of statistical ray-tracing techniques to problems where the non-

random "background" density component is inhomogeneous. It has been found that a strongly refracted beam of light will not only spread due to the random density fluctuations; its mean (center) ray will also drift slightly from the path taken by the unperturbed, zero-fluctuation ray path. To our knowledge, such a drift has never been derived or described in a statistical ray-tracing theory, but it is a necessary part of a quantitatively complete beam-propagation theory. A drift term has been formally expressed in a wave diffusion theory by Carnevale *et al.*,⁹ but this term was not evaluated for circumstances general enough to give a nonzero result for this effect. The development by Komissarov¹⁰ of ray statistics for refracting media is very similar to the one to be presented here, but he ultimately neglects refraction fluctuation terms that could lead to a drift effect.

The calculation of energy absorption efficiencies in the presence of density fluctuations superimposed upon an idealized density profile has been considered elsewhere for coherent disturbances of the density profile¹¹ and for random density fluctuations confined to restricted regions along density gradients near the critical surface where resonance absorption occurs.^{12,13} The formalism to be discussed here deals more directly with the propagation of the light and considers random density fluctuations throughout the plasma, so that the results depend upon the statistical properties of the plasma as a whole, rather than on a restricted class of coherent density ripples or on fluctuations in a restricted region.

To demonstrate the use and validity of statistical ray tracing, results for the evolution of intensity profiles of beams incident on a plane-parallel linear-profile plasma will be presented and compared with numerical Monte Carlo results.

The statistical ray-tracing approach is applicable only to problems where the electron-density profile can be decomposed into a nonfluctuating component and a random component that gives each ray in a beam of light a random perturbation. In hydrodynamic simulation codes,

the light intensity distribution is often computed by tracing an ensemble of rays, ray by ray, through the plasma. The electron-density information from such codes does not include an identification of random and nonfluctuating components, but the statistical ray-tracing method could be useful if such a decomposition could be postulated *ad hoc*. For example, one could model the effects of fluctuations whose scale lengths are too short to be resolved by a computational fluid mesh. In the illustrative example to be considered below, the nonfluctuating, unperturbed density component is represented by an idealized analytic form. This allows the intensity profile of a beam of light to be expressed in terms of the solution of a set of coupled ordinary differential equations. This simplification makes it relatively easy to study the dependence of the evolution of a beam on the statistical parameters of the density fluctuations and on the initial conditions of the beam. A much greater effort would be required to obtain a large data base from Monte-Carlo calculations.

II. STATISTICAL RAY-TRACING THEORY

To calculate the behavior of a statistical ensemble of perturbed ray trajectories, one begins with the ray equation of geometrical optics¹⁴

$$\mu \frac{d}{ds} \mathbf{v} = \nabla \mu - \mathbf{v}(\mathbf{v} \cdot \nabla \mu), \quad (1a)$$

$$\mu = (1 - n_e/n_c)^{1/2} \quad (1b)$$

for the deflection of the ray direction vector \mathbf{v} at a point along the ray trajectory specified by the path-length parameter s . The index of refraction of the plasma is given here in terms of the electron density n_e and the critical electron density n_c in Eq. (1b). The ray equation relates ray-trajectory perturbations to zero-mean density perturbations δn superimposed upon a background density n_0 , where

$$n_e = n_0 + \delta n, \quad (2a)$$

and

$$\langle \delta n \rangle = 0. \quad (2b)$$

The brackets denote a local average. This perturbation approach requires that the rms amplitude of the density fluctuations σ be small so that the relative fluctuations of the index of refraction are small. This condition is

$$\sigma \ll n_c - n_0, \text{ or } \delta \mu / \mu \ll 1, \quad (3a)$$

where

$$\sigma^2 = \langle \delta n^2 \rangle. \quad (3b)$$

The density fluctuations are characterized by a correlation length h that must be much smaller than the overall scale length L of the problem. For the present, a suitable example is

$$\langle \delta n(\mathbf{x}) \delta n(\mathbf{x} + \Delta \mathbf{x}) \rangle = \sigma(\mathbf{x}) \sigma(\mathbf{x} + \Delta \mathbf{x}) \exp(-\Delta \mathbf{x} \cdot \Delta \mathbf{x} / h^2), \quad (4a)$$

where

$$h \ll L \sim n_0 / |\nabla n_0| \sim \sigma^2 / |\nabla \sigma^2|. \quad (4b)$$

This example contains a long-scale-length spatial dependence in addition to the short-scale-length Gaussian cut-off.

By passing an ensemble of rays, all with an initial direction vector \mathbf{v} (or, equivalently, an infinitesimal element of a phase-space distribution) through a large sample of these fluctuations, the following expression for the rate of change of the mean direction vector $\langle \mathbf{v} \rangle$ is obtained:

$$\begin{aligned} \frac{d}{ds} \langle \mathbf{v} \rangle = & - \frac{[\nabla n_0 - \mathbf{v}(\mathbf{v} \cdot \nabla n_0)]}{2(n_c - n_0)} + \frac{[\nabla \sigma^2 - \mathbf{v}(\mathbf{v} \cdot \nabla \sigma^2)]}{8(n_c - n_0)^2} \\ & - \frac{\pi^{1/2}}{2} \frac{\sigma^2}{h(n_c - n_0)^2} \mathbf{v}. \end{aligned} \quad (5)$$

Equation (5) is obtained by integrating Eq. (1a) over a path interval that is small in comparison with the overall scale length of the problem, yet long enough in comparison with the correlation length, so that the nonaccumulating effects of the fluctuations average out. In obtaining Eq. (5), Eqs. (1) and (2) must be iterated at least once for the lowest-order nonzero-fluctuation effects to appear.

The first term in Eq. (5) represents the refraction of the rays due to the unperturbed density gradient. The second term represents an additional drift due to the gradient of the fluctuation amplitude, and the third term represents the foreshortening of the mean direction vector due to the spreading of the individual rays away from the mean direction. The net shift and spreading occur because correlations in the density fluctuations cause the random impulses to fortuitously reinforce each other. It is significant that no drift effect due to the simultaneous presence of density fluctuations and a nonzero-background gradient is found. The slowing term due to the spreading of the beam agrees with the earliest results in ray statistics.^{1,2,10} By removing the slowing term, Eq. (5) becomes an expression for the rate of change of the direction of the mean direction vector, so by making the additional change of substituting \mathbf{v} for $\langle \mathbf{v} \rangle$, Eq. (5) becomes an equation for the trajectory of the mean ray of a beam.

The angular spreading rate of the light beam is obtained by solving Eq. (1a) to lowest order in δn and forming the ensemble average of the square of the ray deflections. This gives

$$\frac{d}{ds} \langle \mathbf{v}_\perp \cdot \mathbf{v}_\perp \rangle = \pi^{1/2} \frac{\sigma^2}{h(n_c - n_0)^2}, \quad (6)$$

which is the growth rate of the mean-square angular radius of the ray distribution. The growth rate is just what one would expect for a random walk in the profile plane, where each ray receives a random angular displacement of roughly $\sigma/(n_c - n_0)$ rad from each independent fluctuation it traverses, or, equivalently, once per correlation length h along its path. The total rms angular displacement is essentially the displacement due to one impulse, or one fluctuation, multiplied by the square root of the number of impulses, just as is indicated by the form of Eq. (6). Equations (5) and (6) are derived in the Appendix.

III. SOLVING AN ILLUSTRATIVE PROBLEM

The problem to be considered below is that of a beam spreading as it refracts through a plane-parallel uniform-gradient plasma. The solution is cast in the form of an elliptical Gaussian ray distribution in the profile plane of the beam. This plane is represented in Fig. 1 by the X - Y axes placed normal to the trajectory of the mean ray, $\mathbf{x}(s)$, at the point denoted by s . The unperturbed trajectory $\mathbf{x}_0(s)$ is assumed to be known from the solution to this problem for $\sigma=0$. The displacement of the mean ray from the unperturbed trajectory can be found by integrating the beam-shift term in Eq. (5). The beam-profile distribution is centered on the mean ray and is represented in Fig. 1 by an isointensity surface, such as the rms beam-radius surface. The evolution equation for this distribution is calculated by propagating each infinitesimal phase-space element of the distribution an infinitesimal distance while allowing each element to broaden at the rate given by Eq. (6). The evolution equation itself and the details of its derivation and solution are presented in the Appendix. The beam-profile intensity distribution can be written in terms of the phase space $(\mathbf{X}_\perp, \mathbf{V}_\perp)$ of the profile plane in the form

$$F(\mathbf{X}_\perp, \mathbf{V}_\perp) \propto \exp \left[- \left(\frac{X^2}{a_X(s)} + \frac{2XY}{b_X(s)} + \frac{Y^2}{c_X(s)} \right) - \left(\frac{Y^2}{a_Y(s)} + \frac{2VY}{b_Y(s)} + \frac{V^2}{c_Y(s)} \right) \right], \quad (7)$$

where either of the principal (X or Y) axes remains parallel to the constant-density surfaces of the unperturbed plasma, and the other principal axis remains in the plane of the mean ray path as the refraction of the mean beam rotates the profile plane. The evolution equation for F reduces to a set of coupled ordinary differential equations for the six parameters in Eq. (7), $a_X(s)$, $a_Y(s)$, etc. For cases without the high degree of symmetry of the plane-parallel problem, there may not be well-defined principal axes of the beam profile, and more terms and parameters may be needed [e.g., $XY/p(s)$, $XV_Y/q(s)$, etc.].

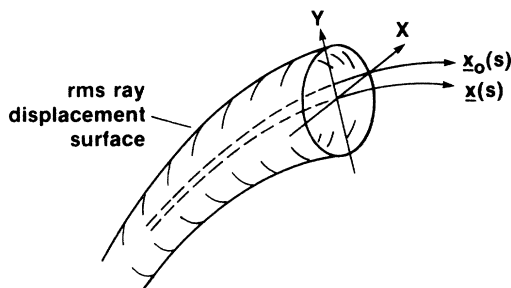


FIG. 1. A statistical description of a light beam consists of an intensity distribution in the phase space transverse to the mean ray trajectory, $\mathbf{x}(s)$, at a point specified by the path-length parameter s . The mean ray is generally shifted from the path of the unperturbed ray, $\mathbf{x}_0(s)$. The beam envelope, defined by the rms displacement of rays from the mean ray along any direction in the profile plane, provides a concrete visualization of the beam.

IV. STATISTICAL AND MONTE CARLO RESULTS FOR THE ILLUSTRATIVE PROBLEM

The plane-parallel plasma considered here is illustrated in Fig. 2 with constant rms amplitudes of 4% and 1% of the critical density. Density fluctuations such as these are generated for the Monte Carlo solutions to this problem. These fluctuations are expressed within the Monte Carlo calculation as a Fourier series with the amplitude of each term set so that the correlation function in Eq. (4a) is obtained from the discrete spectrum with phases taken from a random-number generator. The Fourier components in frequency space are chosen such that the fluctuations and the correlation function are periodic in space with the period chosen to be equal to one scale length L . The electron density is written

$$n_e = (x/L)n_c + \delta n(x, y, z), \quad (8)$$

where

$$\frac{\delta n}{n_c} = \sum_{m=1}^M A_m \sin[(2\pi/L)(p_m x + q_m y + r_m z + \phi_m)], \quad (9a)$$

where P_m , q_m , and r_m are integers specifying one of M different modes, where ϕ_m is the phase of the mode, and where

$$A_m = \frac{2\sigma}{n_c} \left[\frac{\pi^{1/2} h}{L} \right]^{3/2} \exp \left[- \frac{\pi^2 h^2}{2L_c^2} (p_m^2 + q_m^2 + r_m^2) \right]. \quad (9b)$$

The sum in Eq. (9a) is taken over all distinct modes such that the exponential factor in Eq. (9b) exceeds 0.01. At this level, the Monte Carlo results are not changed noticeably by adding more modes to the sum. For typical parameters ($h=0.1, L=1.0$), $M=678$. For a purely 2D calculation (i.e., with $\delta n z$ independent), these criteria

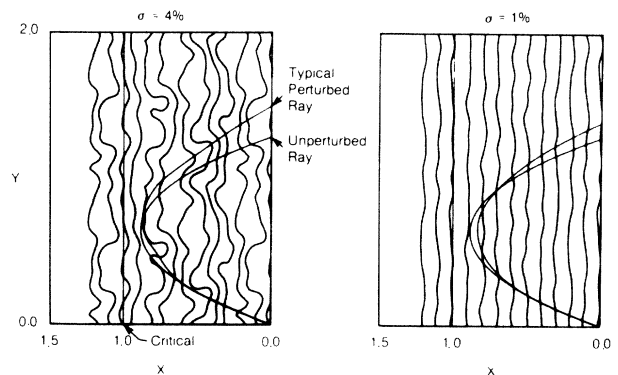


FIG. 2. Plane-parallel uniform-gradient plasmas with superimposed density fluctuations indicated by isodensity contours. Cases with rms fluctuation amplitudes $\sigma/n_c=0.01$ and 0.04 are shown. The correlation length h is chosen to be $h/L=0.1$. The contours of $n_e/n_c = x/L + \delta n(x, y, z)/n_c$ are in intervals of 0.1. Each frame shows how a typical ray wanders from the unperturbed path due to the given fluctuations.

would give $M = 72$. The correlation length in the example of Fig. 2 is chosen to be $h/L = 0.1$. Each frame shows how a typical ray wanders from the unperturbed path due to these fluctuations.

Figure 3 shows how 49 different rays propagate through these same two plasmas. For each ray, the phases of the Fourier components are changed by shifting the density perturbations δn relative to the starting point of the beam by amounts corresponding to a uniform sampling of the unit cube of side L . The rms spatial widths of these beams calculated according to the statistical ray-tracing method can be used to construct the rms beam envelope. The boundaries of this envelope in the plane of refraction of the unperturbed ray are drawn in Fig. 4 so that Figs. 3 and 4 can be compared by superposition. Most of the Monte Carlo rays lie within the rms boundaries. It is interesting to note that qualitative features, such as the focusing of the beam just after the turning point, are reproduced. This focusing by the background density gradient gives the beam an elliptical profile. Earlier statistical results predicting a circular beam distribution for a similar problem are incorrect.¹⁰

A more quantitative comparison of the Monte Carlo and statistical methods is shown in Fig. 5 where the rms angular radii (at the point of emerging from the plasma) are plotted as functions of the angle of incidence. The emerging beam profile is elliptical with principal axes in and normal to the unperturbed plane of refraction. Here, $\sigma/n_c = 0.01$ and $h/L = 0.1$. The scatter of the Monte Carlo points is due to the limited number (27) of trials taken per run. The agreement of these points with the statistical theory curves is well within this scatter. The spatial width of the emerging beam obtained by both methods is plotted in Fig. 6, where the agreement between the statistical curve and the scattered Monte Carlo points is also apparent. The isolated X in both Figs. 5 and 6 represents a statistical result for the singular normal-incidence case. As the initial beam approaches normal incidence, the distance of closest approach to the critical surface of the unperturbed ray path becomes smaller, and

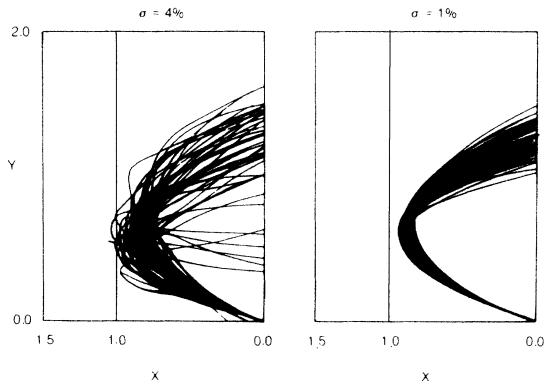


FIG. 3. Bundles of 49 rays propagating in the same conditions illustrated in Fig. 2. Each ray shown propagates according to a statistically independent sample of the fluctuation distribution. The bundles are Monte Carlo representations of a spreading beam.

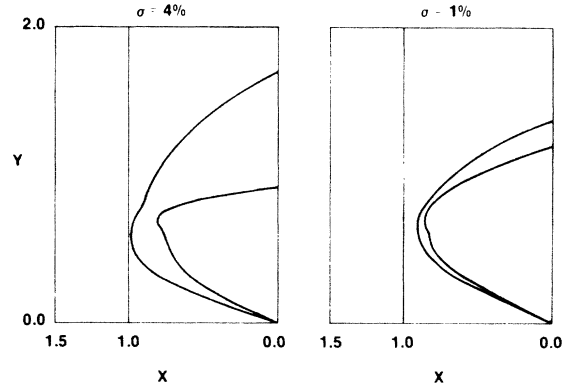


FIG. 4. The outlines of the rms ray-displacement envelopes obtained from the statistical ray-tracing theory for the same conditions as in Figs. 2 and 3. The agreement between the statistical and Monte Carlo calculations is apparent from the superposition of the corresponding frames of Figs. 3 and 4.

the small-perturbation condition, Eq. (3a), is eventually violated. The calculation of the isolated normal-incidence point avoids this difficulty by simply neglecting any beam spreading that occurs within one correlation length of the unperturbed critical surface. This *ad hoc* "fix up" affects only a small fraction of the total ray path, so it is not un-

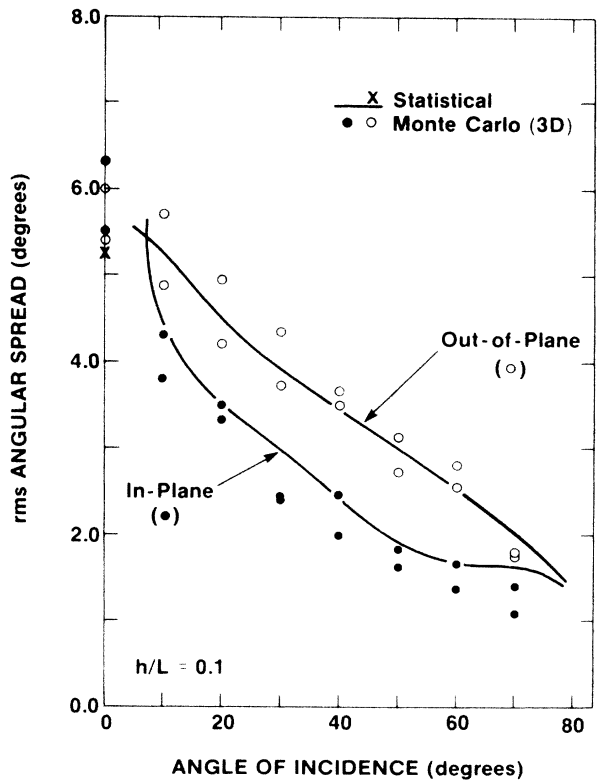


FIG. 5. The principal rms angular radii of the elliptical profile of the beam (at the point where it emerges from the slab) are plotted as functions of the angle of incidence of the initial pencil beam. The conditions $\sigma/n_c = 0.01$ and $h/L = 0.1$ are assumed. The statistical ray-tracing results fall within the scatter of the dots representing Monte Carlo calculations.

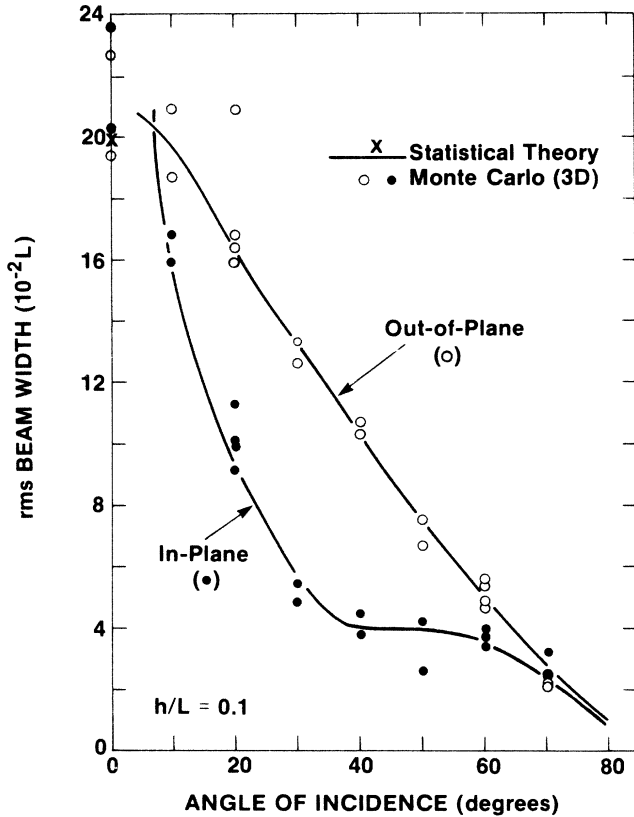


FIG. 6. Same as Fig. 5, except that the principal rms spatial radii, rather than angular radii, are plotted.

reasonable that the statistical result should be in rough agreement with the Monte Carlo results.

According to the σ scaling of the angular spreading rate given by Eq. (6), the angular and spatial widths given in Figs. 5 and 6 should scale linearly with σ . This scaling is verified in Fig. 7 for the spatial beam width in the plane

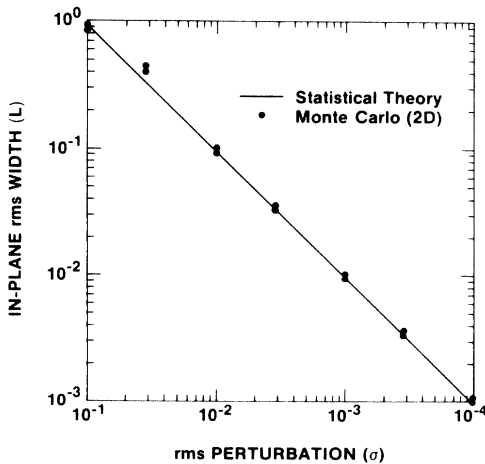


FIG. 7. The rms width, in the unperturbed plane of refraction, of the emerging beam plotted as a function of the rms density-fluctuation amplitude for an angle of incidence of 20° and for $h/L = 0.1$. The predicted linear scaling of the beam width with the fluctuation amplitude is verified by Monte Carlo calculations, up to a fluctuation level of $\sigma/n_c = 0.1$.

of refraction for an angle of incidence of 20° . The Monte Carlo runs verify this linear scaling up to a fluctuation level of $\sigma/n_c \sim 0.1$. At the point along the unperturbed ray most closely approaching the critical surface, density fluctuations of this magnitude typically give index-of-refraction fluctuations comparable to the unperturbed index of refraction, which violates the small-perturbation condition, Eq. (3b). The verification of linear scaling for such large fluctuation amplitudes is a strong indication of the reliability of the statistical method, even when the small-parameter conditions are strained.

It has been observed experimentally that angle-of-incidence dependences of energy absorption efficiencies are weaker than predicted by simple analytical models.¹² In some cases, such an effect may be attributable to density fluctuations. Figure 8 shows the absorption fraction for inverse bremsstrahlung for the plane-parallel uniform-gradient plasma considered above, plotted as a function of the angle of incidence. The circles represent individual two-dimensional Monte Carlo calculations for $\sigma/n_c = 0.05$ and $h/L = 0.1$. These are to be compared with the solid curve obtained analytically for the $\sigma = 0$ case.¹⁵ For an isothermal unperturbed plasma, the absorption fraction A is evaluated by integrating

$$A = 1 - \exp \left[- \int \frac{\kappa_0 (n_e/n_c)^2}{(1 - n_e/n_c)^{1/2}} ds \right] \quad (10)$$

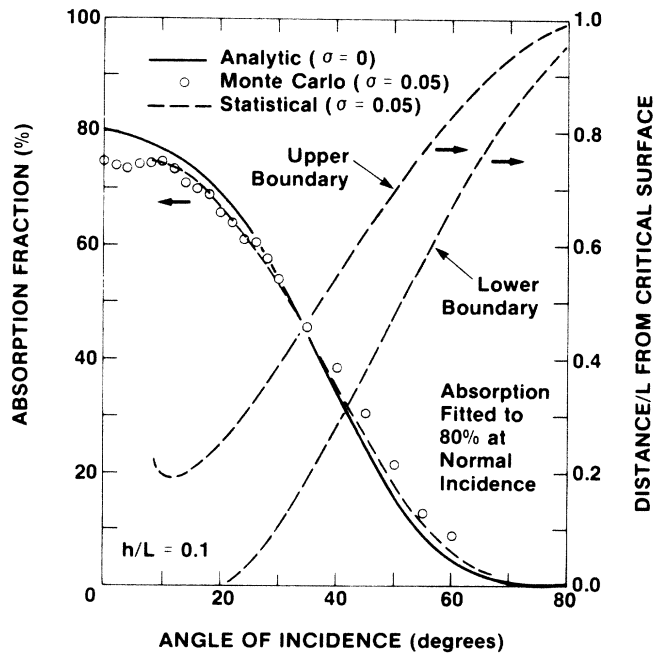


FIG. 8. Monte Carlo (circles) and statistical ray-tracing (dashed curve) estimates of the inverse-bremsstrahlung absorption fraction are plotted (left-hand scale) as functions of the angle of incidence for the $\sigma/n_c = 0.05$, $h/L = 0.1$ case. The absorption coefficient is chosen to give 80% absorption at normal incidence for the $\sigma = 0$ result shown by the solid curve. The statistical estimate of the absorption is obtained using penetration-depth distribution results represented by the upper-boundary and lower-boundary curves (right-hand scale).

along the ray path, which takes into account the density dependence of the electron-ion collision frequency and the group velocity of the light. In these calculations, the absorption coefficient κ_0 was set such that 80% absorption would be obtained for normal incidence with $\sigma=0$. The pair of dashed curves, read with the right-hand scale, gives the statistical theory results for the upper and lower rms beam boundaries at the point of closest approach to the critical surface, as a function of angle of incidence. The leveling of the Monte Carlo angular dependence occurs at angles of incidence below about 15° , roughly where the statistical theory predicts a significant concentration of rays grazing the critical surface, a region accessible only to normally incident rays in an unperturbed plasma. Further decreases in the angle of incidence do not increase the concentration of near-critical rays significantly, just as if the beam were incident on the unperturbed plasma with an initial angular radius of about 15° .

The dashed absorption curve in Fig. 8 is a simple statistical-theory estimate of the change in the absorption efficiency due to the given fluctuations. Since the inverse-bremsstrahlung absorption cross section increases rapidly with electron density, it is assumed that the energy absorbed from a ray is most strongly dependent on the maximum penetration depth and less sensitive to the shape of the path, as long as the perturbed paths remain reasonably smooth. The statistical estimate is obtained by convolving the analytical zero-fluctuation result with a penetration-depth distribution obtained from the statistical calculations. As can be seen in Fig. 8, this statistical estimate gives results similar to the Monte Carlo results. The crudeness of the quantitative agreement is not unexpected, given the simplicity of the estimate. Nevertheless, both the statistical and Monte Carlo calculations give curves that cross the zero-fluctuation result near a 35° angle of incidence, and the distinct flattening of the angle-of-incidence dependence of the statistical results occurs very near where Monte Carlo results suggest. Closer agreement would certainly be obtained by making fuller use of the statistical ray distribution over the entire path of the spreading beam. This has yet to be done. It should be emphasized, however, that the statistical absorption-efficiency results are encouraging as examples of what can be obtained using relatively simple estimates, without resorting to lengthy Monte Carlo calculations.

V. CONCLUSIONS

In this work, statistical ray-tracing techniques have been extended to strongly refracting plasmas. The agreement obtained between the statistical and Monte Carlo methods verifies the reliability of the statistical results. It should be noted that density fluctuations as small as a few percent of the critical density with about ten correlation lengths per scale length can result in angular spreads in reflected beams of the order of 10° . The statistical method offers a means to obtain estimates of density fluctuation effects that are otherwise obtainable only by time-consuming Monte Carlo methods. Finally, although we have concentrated on laser-fusion applications, it should be stressed that theories of wave propagation in random

media are of general applicability. The work we have presented is potentially applicable to a number of other areas.

ACKNOWLEDGMENTS

The authors are pleased to thank Edward A. Williams and Alex Friedman for valuable discussions. This work was supported by the Laser Fusion Feasibility Project at the Laboratory for Laser Energetics, which has the following sponsors: Empire State Electric Energy Research Corporation, General Electric Company, New York State Energy Research and Development Authority, Northeast Utilities Service Company, Ontario Hydro, Southern California Edison Company, The Standard Oil Company, and the University of Rochester.

APPENDIX: DETAILS OF THE STATISTICAL-RAY-TRACING FORMALISM

Angular spreading rate

The solution to the ray equation, Eq. (1), in the presence of density fluctuations, such as those described by Eqs. (2)–(4), is

$$v^i(\tau) = v^i(0) - \frac{1}{2} \int_0^\tau \frac{\delta^{ij} - v^i(s)v^j(s)}{n_c - n_0(s) - \delta n(\mathbf{x}(s))} \times [\nabla_j n_0(s) + \nabla_j \delta n(\mathbf{x}(s))] ds, \quad (\text{A1})$$

where τ is a distance along the ray path that is small in comparison with the overall scale length of the problem, yet long enough for the nonaccumulating effects of the density fluctuations to average out. This represents an intermediate scale length for which we assume

$$h \ll \tau \ll L. \quad (\text{A2})$$

The index notation for vectors and tensors is adopted for the Appendix ($i = x, y, \text{ or } z$, repeated indices are summed, and δ^{ij} is the Kronecker δ or the unit dyad). To leading order in δn , we have

$$[v^i(\tau) - v_0^i(\tau)] - [v^i(0) - v_0^i(0)] = - \frac{\delta^{ij} - v_0^i(0)v_0^j(0)}{2[n_c - n_0(0)]} \int_0^\tau \nabla_j \delta n(s) ds \quad (\text{A3})$$

for the deviation of the perturbed ray from the unperturbed direction. Since fluctuations vary over the scale length h , which is the smallest relevant scale length, the nongradient fluctuation terms have been neglected in Eq. (A3). The velocity $v_0^i(s)$ is the unperturbed ray direction. Equation (A1) shows explicitly that δn in the integrand is to be evaluated at points in space along the perturbed path, not the unperturbed path. This distinction can be disregarded in calculating the leading-order spreading rate, but it will become important in the next section.

The angular spreading rate for an ensemble or beam of rays is the tensor square of $\Delta v^i(\tau)$ averaged over an ensemble of fluctuations along the path of the mean ray which, to an adequate approximation, is the path along the initial ray direction. This gives

$$\begin{aligned} \langle \Delta v^i \Delta v^j \rangle_\tau &= \frac{P^{ik} P^{jl}}{4(n_c - n_0)^2} \left\langle \left[\int_0^\tau \nabla_k \delta n(s) ds \right] \right. \\ &\quad \left. \times \left[\int_0^\tau \nabla_l \delta n(s') ds' \right] \right\rangle, \end{aligned} \tag{A4}$$

where the transverse projection operator

$$P^{ij}(s) = \delta^{ij} - v_0^i(s) v_0^j(s) \tag{A5}$$

simplifies the notation. The gradient operates only on the

$$\begin{aligned} \int_0^\tau \int_0^\tau \langle f(t) g(t') \rangle dt dt' &= \int_0^\tau \left[(\tau - s) \langle f(t_0) g(t_0 + s) \rangle + \langle f(t_0) g(t_0 - s) \rangle \right] \\ &\quad + \frac{s(\tau - s)}{2} \left[\frac{d}{dt_0} \langle f(t_0) g(t_0 - s) \rangle - \frac{d}{dt_0} \langle f(t_0) g(t_0 + s) \rangle \right] ds, \end{aligned} \tag{A7a}$$

where

$$t_0 = \tau/2. \tag{A7b}$$

It is assumed that the correlation function $\langle f(t_0) g(t_0 + s) \rangle$ has distinct long-scale (t_0 -dependent) and short-scale (s -dependent) behavior as in the example shown in Eq. (4) so that the approximation

$$\begin{aligned} \langle f(t) g(t - s) \rangle &\simeq \langle f(t_0) g(t_0 - s) \rangle + (t - t_0) \frac{d}{dt_0} \langle f(t_0) g(t_0 - s) \rangle \end{aligned} \tag{A7c}$$

suffices. For calculating the angular spreading rate, the leading-order terms suffice, and we write, ignoring terms smaller by factors of order h/τ and h/L ,

$$\int_0^\tau \int_0^\tau \langle f(t) g(t') \rangle dt dt' \simeq \tau \int_{-\tau}^\tau \langle f(t_0) g(t_0 + s) \rangle ds. \tag{A8}$$

Using Eq. (A4), this gives

$$\begin{aligned} \frac{\langle \Delta v^i \Delta v^j \rangle}{\tau} &= \frac{P^{ik} P^{jl}}{4(n_c - n_0)^2} \int_{-\tau}^\tau \langle \nabla_k \delta n(t_0) \cdot \nabla_l \delta n(t_0 + s) \rangle ds. \end{aligned} \tag{A9}$$

Equation (A9) gives the instantaneous rate of angular spreading in the neighborhood of $s = t_0$. The limits of the integral are essentially infinite, according to Eq. (A2), so we write

$$\begin{aligned} \langle \delta n_{,i}(\mathbf{x}) \delta n_{,j}(\mathbf{x} + \mathbf{s}) \rangle &= \left[\frac{2}{h^2} (\delta^{ij} - 2s^i s^j) \sigma(\mathbf{x}) \sigma(\mathbf{x} + \mathbf{s}) + \frac{2s^i}{h^2} \sigma(\mathbf{x}) \sigma_{,j}(\mathbf{x} + \mathbf{s}) - \frac{2s^j}{h^2} \sigma_{,i}(\mathbf{x}) \sigma(\mathbf{x} + \mathbf{s}) + \sigma_{,i}(\mathbf{x}) \sigma_{,j}(\mathbf{x} + \mathbf{s}) \right] e^{-s^2/h^2}. \end{aligned} \tag{A12}$$

quantity immediately following it. All unperturbed quantities written without the path-length parameter are understood to be evaluated at $s = 0$. A simple rearrangement gives

$$\begin{aligned} \left\langle \left[\int_0^\tau \nabla_k \delta n(s) ds \right] \cdot \left[\int_0^\tau \nabla_l \delta n(s') ds' \right] \right\rangle &= \int_0^\tau \int_0^\tau \langle \nabla_k \delta n(s) \cdot \nabla_l \delta n(s') \rangle ds ds'. \end{aligned} \tag{A6}$$

This double integral can be reduced to a single integral over correlation functions by using the relation

$$\begin{aligned} \frac{d}{ds} \langle \Delta v^i \Delta v^j \rangle &= \frac{P^{ik} P^{jl}}{4(n_c - n_0)^2} \int_{-\infty}^\infty \langle \nabla_k \delta n(t_0) \cdot \nabla_l \delta n(t_0 + s) \rangle ds \end{aligned} \tag{A10}$$

for the tensor rate of angular spreading in terms of the correlation function for the gradients of the density fluctuation.

Equation (A10) is now evaluated in terms of the chosen density fluctuations specified by Eq. (4a). The correspondences between the path-parameter arguments of the correlation function in Eq. (A10) and the spatial positions in Eq. (4a) are assumed to be

$$\mathbf{x} = \mathbf{v}_0 t \tag{A11a}$$

and

$$\Delta \mathbf{x} = \mathbf{v}_0 s. \tag{A11b}$$

This use of straight path segments to approximate the actual curved path of the mean ray is valid because the actual and approximate paths differ by very little over the path segment where the integrand is significant, and the statistical properties of the fluctuations being sampled differ negligibly over distances that would separate the actual and linear paths. To simplify the notation, $\mathbf{v}_s \equiv \mathbf{s}$ will be used, and a comma before a vector subscript will denote partial differentiation with respect to a spatial coordinate (e.g., $f_{,i} \equiv \partial f / \partial x^i$). From Eq. (4a), one obtains

The path integral of this quantity is

$$\begin{aligned} & \int_{-\infty}^{\infty} \langle \delta n_{,i}(\mathbf{x}) \delta n_{,j}(\mathbf{x} + \mathbf{s}) \rangle ds \\ &= \frac{2\pi^{1/2}\sigma^2}{h} P^{ij} + 2\sigma(\delta^i v_0^j \sigma_{,i} + v_0^i \sigma_{,j} - v_0^j \sigma_{,i} \\ & \quad - 2v_0^i v_0^j v_0^k \sigma_{,i}) , \end{aligned} \quad (\text{A13})$$

which is used with Eq. (A10) to obtain

$$\frac{d}{ds} \langle \Delta v^i \Delta v^j \rangle = \frac{\pi^{1/2}\sigma^2}{2h(n_c - n_0)^2} P^{ij} . \quad (\text{A14})$$

The leading-order $\sigma_{,i}$ terms in Eq. (A13) are shown for reference but are discarded in Eq. (A14) because they make a negligible (down by order $\sim h/L$) contribution to the spreading-rate tensor, comparable to terms neglected in writing Eq. (A8). Because of the transverse projection property

$$P^{ij} v_0^j = 0 \quad (\text{A15})$$

(recall that repeated indices are summed), the spreading-rate tensor is nonzero only in the plane transverse to \mathbf{v}_0 . This implies the identity

$$\frac{d}{ds} \langle \Delta v^i \Delta v^i \rangle = \frac{d}{ds} \langle \mathbf{v}_1 \cdot \mathbf{v}_1 \rangle , \quad (\text{A16})$$

which, with Eq. (A14) and the property

$$P^{ii} = 2 , \quad (\text{A17})$$

gives Eq. (6).

Equation for the mean-ray direction vector

The derivation of Eq. (5) resembles the derivation of Eq. (4) in many formal respects, particularly in that we are led to an intermediate result given entirely in terms of correlation functions of the density fluctuations. Considerably more work is involved, however, because the con-

tributions of terms of nonleading order in the small parameters σ/n_c and h/L must be kept. Again, we begin with Eq. (A1), this time respecting the distinction between density fluctuations along the perturbed and unperturbed paths. The density fluctuation can be written in terms of the fluctuation along the unperturbed path as

$$\delta n(\mathbf{x}(s)) \simeq \delta n(\mathbf{x}_0(s)) + [\mathbf{x}(s) - \mathbf{x}_0(s)] \cdot \nabla \delta n(\mathbf{x}_0(s)) . \quad (\text{A18})$$

This linear expansion is valid as long as the perturbed and unperturbed paths are separated at any given value of s by much less than one correlation length. The order of magnitude of this separation after a propagation distance $s \lesssim \tau$ can be obtained from Eq. (6), which gives for this condition

$$|\mathbf{x}(\tau) - \mathbf{x}_0(\tau)| \sim \sigma \tau^{3/2} / h^{1/2} \ll h , \quad (\text{A19})$$

which can be written as a restriction on the amplitude of the density fluctuations

$$\sigma \ll (h/\tau)^{3/2} . \quad (\text{A20})$$

As was stated in the main text, Eq. (5) is obtained from Eq. (1) by averaging the solution Eq. (A1) over the ensemble of density fluctuations. The integral in Eq. (A1) must first be written entirely in terms of the path of the unperturbed ray and the density fluctuations along the unperturbed path and then expanded at least through second order in the density fluctuations. The lowest-order accumulating effects of the density fluctuations will be ensemble averages of these second-order terms that are linear in τ . Over the length of the ray path, the approximation

$$n_0(s) \simeq n_0(0) + s v_0^i(0) \nabla_i n_0(0) \quad (\text{A21})$$

is used. Corrections due to the curvature of the unperturbed path or deviations of the perturbed path from the unperturbed path are negligible. The velocity appropriate for iterating into the transverse projection operator in Eq. (A1) is

$$v^i(s) = v_0^i(s) - \frac{P^{ij}}{n_c - n_0(0)} \int_{-\infty}^s \left[\nabla_j \delta n(t) + \nabla_j n_0 \left[1 + \frac{t^k \nabla_k n_0 + \delta n(t)}{n_c - n_0(0)} + \frac{[t^k \nabla_k n_0 + \delta n(t)]^2}{[n_c - n_0(0)]^2} \right] \right] dt . \quad (\text{A22})$$

The needed expansion of Eq. (A1) is obtained by substituting Eqs. (A18), (A21), and (A22) into Eq. (A1). The expression for the perturbation of the ray path needed to evaluate Eq. (A18) is the integral of the first-order fluctuation terms of Eq. (A22),

$$\mathbf{x}^i(s) - \mathbf{x}_0^i(s) = - \frac{P^{ij}}{2[n_c - n_0(0)]} \int_{-\infty}^s \int_{-\infty}^t \left[\frac{\delta n(u) \nabla_j n_0(u)}{n_c - n_0(0)} + \nabla_j \delta n(u) \right] du dt . \quad (\text{A23})$$

The result is

$$\begin{aligned} \langle v^i(\tau) - v^i(0) \rangle = & - \frac{P^{ij} \nabla_j n_0}{2(n_c - n_0)} \left[\tau + \frac{1}{(n_c - n_0)} \int_0^\tau \langle \delta n(s)^2 \rangle ds \right. \\ & - \frac{P^{kl}}{2(n_c - n_0)} \left[\nabla_l n_0 \int_0^\tau \int_{-\infty}^s \int_{-\infty}^t \langle \nabla_k \delta n(s) \cdot \delta n(u) \rangle du dt ds \right. \\ & \left. \left. + \int_0^\tau \int_{-\infty}^s \int_{-\infty}^t \langle \nabla_k \delta n(s) \cdot \nabla_l \delta n(u) \rangle du dt ds \right] \right] \end{aligned}$$

$$\begin{aligned}
& -\frac{P^{ij}}{2(n_c - n_0)^2} \left[\frac{1}{2} \int_0^\tau \nabla_j \langle \delta n(s)^2 \rangle ds \right. \\
& \quad + P^{kl} \left[\frac{\nabla_l n_0}{(n_c - n_0)} \int_0^\tau \int_{-\infty}^s \int_{-\infty}^u \langle \nabla_k \nabla_j \delta n(s) \cdot \delta n(u) \rangle du dt ds \right. \\
& \quad \quad \left. + \int_0^\tau \int_{-\infty}^s \int_{-\infty}^u \langle \nabla_k \nabla_j \delta n(s) \cdot \nabla_l \delta n(u) \rangle du dt ds \right] \Bigg] \\
& - \left[\frac{v^i(0)P^{jk} + v^j(0)P^{ik}}{4(n_c - n_0)^2} \right] \left[\int_0^\tau \int_{-\infty}^s \langle \nabla_k \delta n(t) \cdot \nabla_j \delta n(s) \rangle dt ds \right. \\
& \quad + \frac{\nabla_k n_0 \nabla_j n_0}{(n_c - n_0)^2} \int_0^\tau \int_{-\infty}^s \langle \delta n(s) \cdot \delta n(t) \rangle dt ds \\
& \quad + \frac{\nabla_k n_0}{(n_c - n_0)} \int_0^\tau \int_{-\infty}^s \langle \nabla_j \delta n(s) \cdot \delta n(t) \rangle dt ds \\
& \quad \left. + \frac{\nabla_j n_0}{(n_c - n_0)} \int_0^\tau \int_{-\infty}^s \langle \nabla_k \delta n(t) \cdot \delta n(s) \rangle dt ds \right]. \tag{A24}
\end{aligned}$$

Equation (A24) is written neglecting terms that are obviously higher than first order in τ . These terms represent higher-order iterations of effects already represented by first-order terms, and they will vanish when the limit

$$\frac{d \langle v^i \rangle}{ds} = \lim_{\tau \rightarrow 0} \frac{\langle v^i(\tau) - v^i(0) \rangle}{\tau} \tag{A25}$$

is taken to obtain an equation of the form of Eq. (5). At this point in the discussion, τ is still a finite averaging length. The mean ray has a continuous well-defined path, so it is clear that the mean ray velocity and acceleration are also well-defined over this interval and that the limit indicated in Eq. (A24) must be permitted eventually. In Eq. (A24), τ must be finite in order for the individual rays in the ensemble to experience the net effects of random forces that are correlated over finite distances. The result obtained is an average acceleration that the mean ray experiences over the finite interval. Since nothing physically distinguishes any one point in this interval from another, one is free to use Eq. (A25) to obtain the average acceleration over an infinitesimal portion of the interval.

The integrals in Eq. (A24) can be written in terms of correlation functions of the density fluctuations and their gradients, just as Eq. (A9) was obtained from Eq. (A4). The required integral formulas are

$$\int_0^\tau \int_{-\infty}^t \langle f(t)g(t') \rangle dt' dt = \tau \int_0^\infty \langle f(\tau/2)g(\tau/2-s) \rangle ds \tag{A26a}$$

and

$$\int_0^\tau \int_{-\infty}^t \int_{-\infty}^{t'} \langle f(t'')g(t) \rangle dt'' dt' dt = \tau \int_0^\infty s \langle f(\tau/2)g(\tau/2-s) \rangle ds, \tag{A26b}$$

where Eqs. (A7b) and (A7c) have been used. These formulas are used with Eq. (A24) to obtain the more useful expression

$$\begin{aligned}
\frac{\langle v^i(\tau) - v^i(0) \rangle}{\tau} = & -\frac{P^{ij} \nabla_j n_0}{2(n_c - n_0)} \left[1 + \frac{1}{(n_c - n_0)\tau} \int_0^\tau \langle \delta n(s)^2 \rangle ds \right. \\
& - \frac{P^{kl}}{2(n_c - n_0)} \left[\nabla_l n_0 \int_0^\infty s \langle \delta n(\tau/2) \cdot \nabla_k \delta n(\tau/2-s) \rangle ds \right. \\
& \quad \left. + \int_0^\infty s \langle \nabla_l \delta n(\tau/2) \cdot \nabla_k \delta n(\tau/2-s) \rangle ds \right] \Bigg] \\
& - \frac{P^{ij}}{2(n_c - n_0)^2} \left[\frac{1}{2\tau} \int_0^\tau \nabla_j \langle \delta n(s)^2 \rangle ds + P^{kl} \left[\frac{\nabla_l n_0}{(n_c - n_0)} \int_0^\infty s \langle \delta n(\tau/2) \cdot \nabla_k \nabla_j \delta n(\tau/2-s) \rangle ds \right. \right. \\
& \quad \left. \left. + \int_0^\infty s \langle \nabla_l \delta n(\tau/2) \cdot \nabla_k \nabla_j \delta n(\tau/2-s) \rangle ds \right] \right] \Bigg]
\end{aligned}$$

$$\begin{aligned}
& - \left[\frac{v^i(0)P^{jk} + v^j(0)P^{ik}}{4(n_c - n_0)^2} \right] \left[\int_0^\infty \langle \nabla_j \delta n(\tau/2) \cdot \nabla_k \delta n(\tau/2 - s) \rangle ds \right. \\
& + \frac{\nabla_k n_0 \cdot \nabla_j n_0}{(n_c - n_0)^2} \int_0^\infty \langle \delta n(\tau/2) \cdot \delta n(\tau/2 - s) \rangle ds \\
& + \frac{\nabla_k n_0}{(n_c - n_0)} \int_0^\infty \langle \nabla_j \delta n(\tau/2) \cdot \delta n(\tau/2 - s) \rangle ds \\
& \left. + \frac{\nabla_j n_0}{(n_c - n_0)} \int_0^\infty \langle \delta n(\tau/2) \cdot \nabla_k \delta n(\tau/2 - s) \rangle ds \right]. \quad (\text{A27})
\end{aligned}$$

To obtain Eq. (5) from Eq. (A27) requires Eq. (4a) plus various intermediate results such as Eqs. (A12) and (A13). The various correlation functions are obtained from Eq. (4a) and the identities

$$\langle f(\mathbf{x})g_{,i}(\mathbf{x}+\mathbf{s}) \rangle = \frac{\partial}{\partial s^i} \langle f(\mathbf{x})g(\mathbf{x}+\mathbf{s}) \rangle \quad (\text{A28a})$$

and

$$\begin{aligned}
\langle f(\mathbf{x})g_{,i}(\mathbf{x}+\mathbf{s}) \rangle + \langle f_{,i}(\mathbf{x})g(\mathbf{x}+\mathbf{s}) \rangle \\
= \frac{\partial}{\partial x^i} \langle f(\mathbf{x})g(\mathbf{x}+\mathbf{s}) \rangle. \quad (\text{A28b})
\end{aligned}$$

From this point it is tedious but straightforward to obtain Eq. (5). Equation (5) includes all terms within the first two leading orders in the small parameter h/L .

Evolution of the beam profile

The purpose of this final section is to describe the evolution of the beam profile by deriving the equations for the evolution of the six parameters in the profile distribution given by Eq. (6). As the beam propagates over an infinitesimal path length Δs along its mean path, the profile distribution spreads and focuses according to a propagator

$$\begin{aligned}
F(\mathbf{X}, \mathbf{V}, s + \Delta s) \\
= \int \int G(\mathbf{X}, \mathbf{V}; \mathbf{X}', \mathbf{V}'; \Delta s) F(\mathbf{X}', \mathbf{V}', s) d^2 X' d^2 V', \quad (\text{A29})
\end{aligned}$$

where

$$\begin{aligned}
G(\mathbf{X}, \mathbf{V}; \mathbf{X}', \mathbf{V}'; \Delta s) \\
= G_0 \lim_{\epsilon \rightarrow 0} \exp \left[\frac{|\mathbf{X} - \mathbf{V}' \Delta s - \mathbf{X}'|^2}{\epsilon} \right] \\
\times \exp \left[\frac{|\mathbf{V} - \mathbf{V}' - \mathbf{A} \cdot \mathbf{X}' \Delta s - \mathbf{B} \cdot \mathbf{V}' \Delta s|^2}{\gamma \Delta s} \right], \quad (\text{A30})
\end{aligned}$$

where vector components are expressed relative to the profile-plane coordinates, and where G_0 is a constant chosen so that this propagator conserves rays. The first exponential factor is a form of the δ function chosen to

facilitate the use of Eq. (A29) with Eq. (7) by reducing the integral to a simple convolution of Gaussian functions. This first factor propagates each infinitesimal element of the beam distribution over the step Δs according to its original velocity \mathbf{V}' . The second exponential factor spreads each element of the velocity distribution according to the spreading rate

$$\gamma = \pi^{1/2} \frac{\sigma^2}{h(n_c - n_0)^2} \quad (\text{A31})$$

given by Eq. (6). The quantities \mathbf{A} and \mathbf{B} represent focusing terms. The force of these terms is linear in the phase-space separation of a given ray from the mean ray. A real force arises from the spatial and directional dependence of the refractive acceleration due to the background density gradient, and a pseudoforce arises from the rotation of the reference frame of the profile plane as it follows the mean ray. It is these focusing terms that allow the statistical theory to reproduce the elliptical beam profile and the focusing of the beam seen in Fig. 3 just past the turning point of the beam. The ray-statistical equations of Komissarov do not include the phase-spatial dependence of the refractive force due to the background refractive index.¹⁰ Consequently, his solution for a spreading beam refracting in a uniform refractive-index background gradient does not give an elliptical beam profile, which is incorrect.

To obtain the focusing terms, first consider the separation $\mathbf{X}(s)$ in the profile plane between the points of intersection of the mean ray $\mathbf{x}_1(s)$ of the entire distribution and a second ray $\mathbf{x}_2(s')$,

$$\mathbf{X}(s) \equiv \mathbf{x}_2(s') - \mathbf{x}_1(s). \quad (\text{A32})$$

Since the profile plane is normal to the motion of the mean ray, we have

$$\mathbf{v}_1(s) \cdot \mathbf{X}(s) = 0. \quad (\text{A33})$$

At an initial point s , one can set $s' = s$. Over the interval $(s, s + \Delta s)$, $s' - s$ continually changes as the profile plane rotates, staying normal to $\mathbf{v}_1(s)$ as it follows the mean ray. If the trajectories $\mathbf{x}_1(s)$ and $\mathbf{x}_2(s)$ are known, then Eqs. (A32) and (A22) determine $\mathbf{X}(s)$. The position of the intersection of the second ray with the profile plane is re-

ferred to the profile plane coordinates using the unit basis vectors

$$\hat{\mathbf{e}}_X(s) = \frac{\mathbf{a}_1(s) \times \mathbf{v}_1(s)}{|\mathbf{a}_1(s)|} \quad (\text{A34a})$$

and

$$\hat{\mathbf{e}}_Y(s) = -\frac{\mathbf{a}_1(s)}{|\mathbf{a}_1(s)|}, \quad (\text{A34b})$$

which are directions out of and in the plane that momentarily contains the arc of the path of the mean ray. The trajectories $\mathbf{x}_1(s)$ and $\mathbf{x}_2(s)$ [and their respective velocities $\mathbf{v}(s)$ and accelerations $\mathbf{a}(s)$] are obtained from Eqs. (1a) and (1b). The fluctuation-induced corrections to the path of the mean ray given by Eq. (5) make a small and qualitatively uninteresting contribution to the focusing effect.

If one sets path parameters such that $[\mathbf{x}_1(s_0) - \mathbf{x}_2(s_0)]$ is in the profile plane, then

$$\begin{aligned} \mathbf{V}(s_0 + \Delta s) &\simeq \frac{d}{ds} \mathbf{X}(s_0 + \Delta s) \\ &= \mathbf{V}(s_0) + [\mathbf{X}(s_0) \cdot \nabla_X] \mathbf{a}_1(s_0) \Delta s \\ &\quad + [\mathbf{V}(s_0) \cdot \nabla_V] \mathbf{a}_1(s_0) \Delta s \\ &\quad - [\mathbf{v}_1(s_0) + 2\mathbf{a}_1(s_0) \Delta s][\mathbf{a}_1(s_0) \cdot \mathbf{X}(s_0)] \quad (\text{A35}) \end{aligned}$$

is the expression obtained for the mean velocity of a pencil of rays, projected on the profile plane at the point of intersection of the pencil with the profile plane, at a point along the mean trajectory of the entire distribution near the initial point s_0 , where the initial phase-space position of the displaced pencil is given by $[\mathbf{X}(s_0), \mathbf{V}(s_0)]$. The components of $\mathbf{V}(s_0 + \Delta s)$ relative to the profile-plane coordinate system are obtained with the unit vectors given by Eqs. (A34) which we rewrite as

$$\hat{\mathbf{e}}_{X,Y}(s_0 + \Delta s) = \hat{\mathbf{e}}_{X,Y}(s_0) + \Delta s \frac{d}{ds} \hat{\mathbf{e}}_{X,Y}(s_0). \quad (\text{A36})$$

By identifying the $\mathbf{V}(s_0 + \Delta s)$ thus obtained as

$$\mathbf{V}(s_0 + \Delta s) = \mathbf{V}(s_0) + [\mathbf{A} \cdot \mathbf{X}(s_0) + \mathbf{B} \cdot \mathbf{V}(s_0)] \Delta s, \quad (\text{A37})$$

terms on the left corresponding to the \mathbf{A} and \mathbf{B} terms on

the right give the needed expressions for \mathbf{A} and \mathbf{B} .

For the specific example of Eq. (8), the unperturbed motion of rays is simple:

$$\mathbf{a} = -\frac{\sin \theta}{2(L-x)} (\sin \theta \hat{\mathbf{e}}_x - \cos \theta \hat{\mathbf{e}}_y), \quad (\text{A38a})$$

$$\mathbf{v} = \cos \theta \hat{\mathbf{e}}_x + \sin \theta \hat{\mathbf{e}}_y, \quad (\text{A38b})$$

and

$$(L-x) \sin^2 \theta = L \sin^2 \theta_0, \quad (\text{A38c})$$

where θ_0 is the angle of incidence of the beam entering the layer at the $n_e=0$ surface. The nonzero focusing terms obtained are

$$A_{YY} = -\frac{3}{4} \frac{\sin^2 \theta}{(L-x)^2} \quad (\text{A39a})$$

and

$$B_{XX} = B_{YY} = \frac{\cos \theta}{2(L-x)}. \quad (\text{A39b})$$

Evaluating Eq. (A29) using Eqs. (7), (A30), and (A39) and taking the limit $\Delta s \rightarrow 0$ gives

$$\frac{da_i}{ds} = \frac{a_i^2}{b_i} \left[\frac{\gamma}{b_i} + 2A_{ii} \right], \quad (\text{A40a})$$

$$\frac{db_i}{ds} = b_i \left[\frac{b_i}{a_i} + \frac{\gamma}{c_i} + \frac{a_i b_i}{c_i} + B_{ii} \right], \quad (\text{A40b})$$

and

$$\frac{dc_i}{ds} = 2 \frac{c_i^2}{b_i} + \gamma + 2B_{ii} c_i \quad (\text{A40c})$$

for $i=X$ or Y , which are a set of coupled ordinary differential equations governing the evolution of the distribution of the form of Eq. (7). The rms quantities of this distribution in terms of the distribution parameters are

$$\langle X_i^2 \rangle_{\text{rms}} = \frac{a_i}{2(1 - a_i c_i / b_i^2)}, \quad (\text{A41a})$$

and

$$\langle V_i^2 \rangle_{\text{rms}} = \frac{c_i}{2(1 - a_i c_i / b_i^2)}. \quad (\text{A41b})$$

- ¹S. Chandrasekhar, *Mon. Not. R. Astron. Soc.* **112**, 475 (1952); V. A. Krasilnikov, *Dokl. Akad. Nauk SSSR* **47**, 482 (1945).
²L. A. Chernov, *Wave Propagation in a Random Medium* (McGraw-Hill, New York, 1960).
³V. I. Tatarskii, *Wave Propagation in a Turbulent Medium* (McGraw-Hill, New York, 1961).
⁴J. Nuckolls, L. Wood, A. Thiessen, and G. Zimmerman, *Nature (London)* **239**, 139 (1972); J. H. Nuckolls, *Phys. Today* **35** (9), 24 (1982).
⁵S. E. Bodner, *J. Fusion Energy* **1**, 221 (1981).
⁶A review with a lengthy bibliography is found in Y. N. Barabanenkov, Yu. A. Kravstov, S. M. Rytov, and V. I. Tatarskii, *Usp. Fiz. Nauk* **13**, 3 (1971) [*Sov. Phys.—Usp.* **13**, 551 (1971)].

- ⁷F. Villars and V. F. Weisskopf, *Phys. Rev.* **94**, 232 (1954).
⁸*Sound Transmission Through a Fluctuating Ocean*, edited by S. M. Flatte (Cambridge University Press, Cambridge, 1979).
⁹M. Carnevale, B. Crosignani, and P. DiPorto, *Phys. Rev. Lett.* **49**, 916 (1982).
¹⁰V. M. Komissarov, *Izv. Vyssh. Uchebn. Zaved. Radiofiz.* **9**, 292 (1966) [*Sov. Radiophys.* **9**, 193 (1966)].
¹¹A. Montes and M. Hubbard, *Plasma Phys.* **21**, 885 (1979).
¹²J. J. Thomson, W. L. Kruer, A. B. Langdon, C. E. Max, and W. C. Mead, *Phys. Fluids* **21**, 707 (1978).
¹³R. Dragila, *Phys. Fluids* **26**, 1682 (1983).
¹⁴L. D. Landau and E. M. Lifshitz, *Electrodynamics of Continuous Media* (Pergamon, New York, 1960), p. 65.
¹⁵J. W. Shearer, *Phys. Fluids* **14**, 183 (1971).